

Deep Learning-Based Intelligent Fibre Modulation Format Recognition in Optically Coupled Modes

Hai-Bo Zhang*

Information and Communication Company,
State Grid Xinjiang Power Co., Ltd,
Urumqi 830002, P. R. China
a3126853@163.com

Xin Wang

Information and Communication Company,
State Grid Xinjiang Power Co., Ltd,
Urumqi 830002, P. R. China
weopiu@163.com

Qing Li

Information and Communication Company,
State Grid Xinjiang Power Co., Ltd,
Urumqi 830002, P. R. China
hzxihu_l@163.com

Meng-Yao Wang

Information and Communication Company,
State Grid Xinjiang Power Co., Ltd,
Urumqi 830002, P. R. China
kx19901028@163.com

Yao-Hua Wei

The School of Engineering,
The University of Edinburgh,
Edinburgh EH93EA, United Kingdom
xwt20021121@outlook.com

*Corresponding author: Hai-Bo Zhang

Received August 16, 2023, revised October 20, 2023, accepted December 23, 2023.

ABSTRACT. *As the support of smart grid, power optical communication network is an important guarantee to ensure the safe and reliable operation of the system. However, optical fibre, as the basic physical carrier of power optical communication network, needs to rely on manual operations such as optical path adjustment and performance monitoring, which cannot meet the demand of full automation of smart grid. Therefore, a novel optical fibre remote coupling technology is proposed, and the corresponding intelligent identification method of modulation format is implemented using a deep learning model. Firstly, three core technologies of fibre optic remote coupling, fibre distribution strategy and intelligent fibre network structure are given so as to achieve the physical layer pathway at the remote site. Then, an optical coupling RF modulation format recognition method based on deep learning is proposed. The features of five modulation formats, namely 2ASK, 2FSK, BPSK, QPSK and LFM, are mathematically derived using the principle of self-coherence. In order to further extend the dynamic range of signal recognition and enhance the correct rate of signal recognition, the data acquired by the oscilloscope is preprocessed and the amplitude statistical histogram is generated. The generated histogram of amplitude statistics is used as an input to the CNN+LSTM model for modulation format recognition. The experimental results show that the proposed method has the highest overall recognition rate of 97.143% in the range of signal-to-noise ratio of -10dB to 15dB, which is conducive to significantly improving the operation and maintenance efficiency of the communication fibre optic network and realizing intelligent operation and maintenance.*

Keywords: smart optical network; optical switching; deep learning; CNN; LSTM

1. **Introduction.** As a new type of modern power grid, the smart grid system involves a variety of advanced technologies such as advanced sensing technology, communication technology, control technology and energy and power [1,2]. In the process of optimizing the power grid, the optimisation of power communication is one of the important improvements of the grid.

In the construction of electric power communication, the hardware technology of electric power communication needs to be considered, and at the present stage, the commonly used communication equipment is optical fibre [3,4], which has the advantages of long communication transmission distance, fast communication transmission speed and low loss. However, fiber optic power communication needs to rely on manual on-site optical path adjustment, performance monitoring and other operations, which is limited by the dispersed location of the site, manual operation inefficiency and other factors, resulting in the slow development of power communication [5,6], therefore, it is necessary to optimize the fiber optic communication technology, so as to optimize the power communication of the electric power communication, to enhance the efficiency of the optical fiber network operation and maintenance of the electric power communication and to realize the intelligent operation and maintenance.

Optical fibre research is mainly carried out at three levels [7,8]: first, theoretical research, to provide theoretical support for the realization of optical switching, such as from the theoretical analysis of the space division, time division, wave division optical switching; second, optical switching device research, the development of related devices for the practical application of optical switching, such as MEMS optical switches, opto-couplers, etc., which makes the optical device appear diversified; third, the study of optical switching methods and systems. At present, there are still several problems in the construction of all-optical network as follows:

(1) Manual fibre hopping. At this stage, the use of optical fibres in electric power communication needs to be collected manually, and the collected data is input into the computer terminal manually. In this process, due to human involvement, the collected

data may have errors, and when manually inputting the data, there is the possibility of inputting the wrong data, the combination of the two errors, resulting in low validity of the data displayed on the computer side of the low value of participation, and even lead to the staff to misjudge the situation of optical fibre in electric power communication. This situation is also known as artificial fibre skipping, and its a common power communication problem at this stage [9,10].

(2) Optical switching patch fibre. This is achieved by using an optical switch structure unit to form a fully switched device. One side of the optical switch is connected to a number of optical fibres for input, and the other side is connected to a number of optical fibres for output. However, the optical switch in the number of fibers is large, the light needs to pass through the optical waveguide coupling region, from which the output, resulting in serious attenuation of the output optical signal strength; on the other hand, due to the limitations of the optical switch structure and operating principle [11], the optical switch can only realize the exchange between any one input fiber and any one output fiber, and can not realize the exchange between the two input fibers, i.e., it is not possible to realize the exchange of all the optical fibers that are accessed to the In other words, it is not possible to achieve any exchange between all the optical fibres connected to the optical switch (including the input fibre and the output fibre), i.e., it is not possible to achieve the "full exchange".

(3) Difficulty in identifying fibre optic modulation formats. In order to train and evaluate models, large amounts of data with accurate labelling are required [12]. However, in fibre optic modulation format identification, obtaining large-scale appropriately labelled data can be challenging. Also, specialists are required to perform data labelling, which requires a significant investment of time and effort. When identifying fibre optic modulation formats, it is crucial to select appropriate features and extract them. However, there is no universal feature extraction method for all fibre modulation formats [13]. Different modulation formats may have different features and therefore require experienced human experts for feature selection and extraction. The main point to note is that fibre optic modulation formats have diversity and variability. However, the diversity and variability of fibre-optic modulation formats pose a challenge to the identification task. In practice, many different modulation formats may be encountered, which may have similarities and overlaps with each other, thus increasing the difficulty of recognition.

Therefore, the research objective of this work is to improve the optical switching technology in the existing power communication network, to establish physical pathways in the actual physical layer thereby solving the problem of manual fibre hopping and to improve the efficiency of all-optical communication. Secondly, in order to solve the difficulty of fibre modulation format recognition, deep learning techniques are used to achieve automatic recognition of optically coupled RF modulation formats.

1.1. Related Work. In the current power communication network, the traditional switch port rate used in the fibre optic communication system limits the increase in the rate of the fibre optic communication network, and increases the complexity and cost of the equipment, and reduces the reliability of the system. To address the above problems, it is known that they can be solved by all-optical communication, and optical switching is the main link in this technology.

When the sub-station fails or adapts to the needs of line planning, it is usually necessary to establish a new data link between the sub-stations or change the connection form of the existing data link, which is one of the main components of the optical switching technology for power communication. The basis of the data link is optical fibre, through which a data transmission channel is formed, thus forming a data link and completing

the data exchange between the sub-stations. The above process consists of the following steps: Step 1, establish the link, the data link needs to have a bidirectional function, which can complete the request and response. Step 2, maintaining the link, when the data link is used by the sub-station, other forms and other sub-stations are prohibited from using the link, and the uniqueness of the data link is maintained. Step 3, remove the link, the termination command is issued by the sub-station at one end, and the sub-station at the other end confirms it to release the use of the data link and release the resources. The most important part of realising the above optical switching process is the link establishment phase, which requires the establishment of a physical pathway in the actual physical layer, and the physical pathway corresponds to the optical pathway channel. And in this paper, a new optical fibre remote coupling technique is explored to achieve the physical layer pathway at the remote site.

Currently, RF modulated format recognition technology is still in a continuous development phase, and most of the recognition schemes are implemented based on feature extraction [14]. However, in the proposed feature extraction schemes, most of the features can only be used for the recognition of several deterministic signals, and are not generalisable for a wider range of signals. In terms of modulation format recognition methods can be divided into two main categories [15]: likelihood function based methods and feature extraction based methods. In the method of likelihood function, it mainly relies on the probability and hypothesis testing parameters to achieve the modulation format recognition of the signal. In this method, it is necessary to pre-set the assumption value of the result and achieve the modulation format recognition classification by selecting the appropriate threshold value, which leads to the difficulty of implementation. Comparatively, in the method of feature extraction, it is only necessary to extract the common feature of the signal from the signal to be measured and use this common feature to identify and classify the signal to be measured. Although, in general the feature extraction based method does not have a high recognition accuracy as the likelihood function based method, the structure of the feature extraction based method is clear, low complexity and easy to implement. Therefore, the feature extraction based method is chosen in this paper.

In recent years, with the rapid development of deep learning, more and better deep learning schemes have been proposed, and the combination of modulated format recognition and deep learning has gradually appeared. Overall, there are two main categories of deep learning based approaches.

(1) Convolutional Neural Network (CNN) based methods. This type of method will input the modulated signal as an image into the CNN, use the convolutional layer to learn the local features of the modulated signal, and then classify it through the fully-connected layer. Zhu et al. [16] proposed a modulation classification method based on ResNet and the visual attention mechanism, which focuses on the relevant part of the features of the modulated signal through the visual attention mechanism to improve the classification accuracy. Top-notch performance was achieved on the RadioML 2018 dataset. However, the method still requires manual feature selection to extract the amplitude and phase features of the modulated signal through a squaring operation. This part of the operation can be learnt automatically with stronger models.

(2) Recurrent Neural Network (RNN) based methods. This type of method will input the modulated signal as a time sequence into the RNN, and use the recurrent layer to learn the temporal features and long-range dependencies to achieve the classification. Zhang et al. [17] designed an end-to-end LSTM model, which can automatically learn the features of complex modulated signals, and achieved good classification performance on various modulation types. However, the LSTM model is sensitive to the length of the signal

sequence and is less effective in classifying long sequences. Optimisation using Attention or temporal convolutional networks can be considered. Having explored only the standard LSTM structure, one can try to design more complex deep learning models to improve the robustness of the model.

1.2. Motivation and contribution. Through the above analysis, it can be seen that there is still room for improvement in the existing deep learning methods in terms of extracting complex features, generalisation performance and model optimisation. A more powerful deep network structure needs to be designed and rigorous model validation needs to be performed to further improve the performance of modulation format recognition.

Therefore, in order to effectively improve the efficiency of communication fibre optic network operation and maintenance and to achieve intelligent operation and maintenance, this work analyses the existing intelligent optical network technologies and uses the histogram of amplitude statistics of RF signals as the input to the deep learning model to achieve the classification and identification of modulation formats. The main innovations and contributions of this work include:

(1) A new optical fibre remote coupling technology is proposed, and the specific implementation method and fibre core configuration model are given. An intelligent optical fibre network structure based on the optical fibre remote coupling technology is established.

(2) We propose to combine a CNN and a Long Short-term Memory (LSTM) network for the recognition of optically coupled RF modulation formats, which can learn the local features of modulated signals, while the LSTM can learn the temporal features of long sequences, and the combination of the two can learn the spatial and temporal features of the signals at the same time. LSTM is more sensitive to temporal relationship, both CNN and LSTM can be used for feature extraction, and the combination can generate more recognisable features and improve classification performance. Combining two different types of networks can enhance the expressiveness and generalisation of the model.

2. Fibre-optic remote coupling technology.

2.1. Problem description. In the current power communication network, the traditional switch port rate used in the optical fibre communication system limits the increase of the optical fibre communication network rate, and increases the equipment complexity and cost, and reduces the system reliability. Therefore, there is a need to improve the optical switching technology so as to improve the all-optical communication.

When the failure of the sub-station or the need to adapt to the line planning, it is usually necessary to establish a new data link between the sub-stations or change the connection form of the existing data link, which is one of the main components of the optical switching technology for power communication [18,19]. The basis of data link is optical fibre, through which a data transmission channel is formed, thus forming a data link and completing the data exchange between sub-stations. The most important thing to realise the above optical switching process is the link establishment phase, which requires the establishment of physical pathways in the actual physical layer, and the physical pathways correspond to the optical channels. And in this paper, a new type of optical fibre remote coupling technology is explored, which can realize the physical layer pathway at the remote site.

2.2. Core technology. Fibre optic remote coupling technology specific implementation requires three core technologies, the specific implementation of the need to set up a longitudinal and transversal matrix board, in the upper and lower layers controlled by

high-precision stepper motors, towing the optical fibre to the specified location, complete the physical coupling of the optical fibre, as shown in Figure 1.

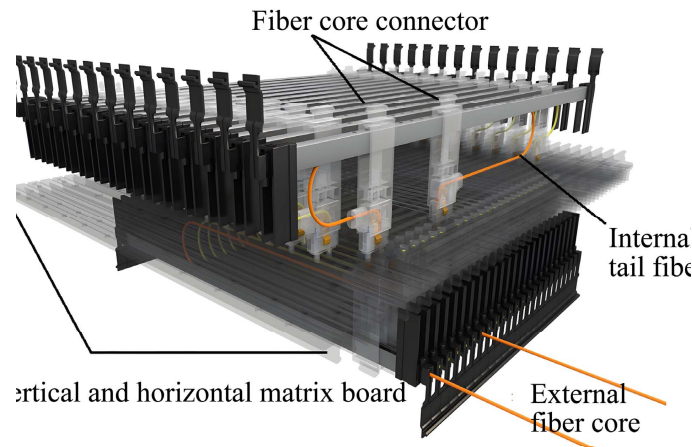


Figure 1. The main structure of the equipment

Its core technology includes the following three aspects: (1) sliding docker; (2) vertical and horizontal switching matrix; and (3) adaptive manipulator. The sliding docker is used to haul external access fibre cores and internal pre-positioned fibre cores, and is the core component to achieve accurate optical fibre docking [20]. The vertical and horizontal switching matrix board distributes parallel-arranged slots on the front and back sides, and there are $N \times N$ docking holes in the slots (N is the maximum number of fibre cores that can be accessed by the device). The manipulator mainly consists of transmission gears, inserters, motors and bearings. The whole set of fibre optic remote coupling device formed by the above technology successfully overcomes the technical difficulties such as remote switching, precise positioning, anti-tailed fibre entanglement, and reduction of insertion loss [21,22].

2.3. Fibre core configuration model. The original optical fibre wiring model mainly connects, distributes and schedules optical fibre lines through optical fibre distribution frames at the end of the local backbone optical fibre in the optical fibre communication system, and its operation is mainly carried out by manual splicing. The fibre optic remote coupling system needs to establish a new set of access standards to solve the problem of fibre core resources when accessing the existing environment.

In view of the state of the fibre optic remote coupling terminal when accessing the fibre core, the relevant fibre core is divided into a total of five categories, as shown in Figure 2. Among them, ① indicates the total number of fibre cores for external access, which can be multiple fibres. ② indicates the number of fibre cores for service hopping. ③ indicates the number of fibre cores for redundancy within the laser acousto-optic deflector (AODF) [23,24]. ④ denotes the number of fibre cores for landed services. ⑤ denotes the number of free fibre cores that are not connected to the fibre core. The weights assigned to different types of fibres are shown in Table 1. Service type weights are shown in Table 2. The rate weights are shown in Table 3. For a service, the sum of its weights = fibre type weights + service type weights + rate weights. For the whole optical fibre weights business ratio = sum of weights of all fibre cores of the optical fibre / number of business cores.

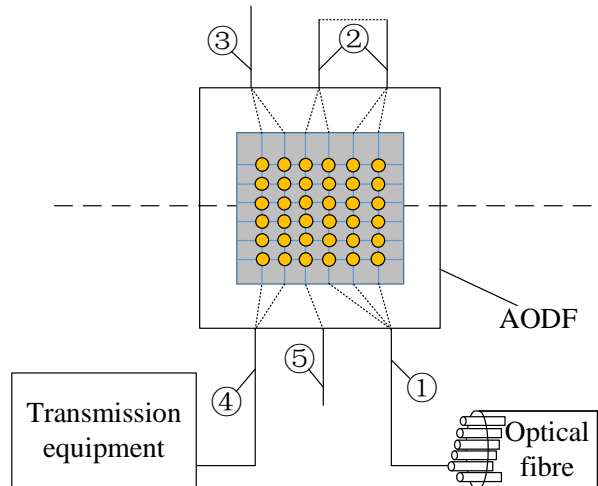


Figure 2. Fibre core configuration model

Table 1. Assignment of weights to different types of fibres

Serial number	Typology	Weighting
1	Optical fibre composite overhead earth wire (OPGW)	1
2	All dielectric self-supporting fibre optics (ADSS)	2
3	Buried common fibre optic	3
4	Overhead common fibre optic	4

Table 2. Service type weights

Serial number	Typology	Weighting
1	HUAWEI	1
2	ECI	2
3	NEC	3
4	data communications network	4

Table 3. Rate weight

Serial number	Rate	Weighting
1	10 G	1
2	2.5 G	4
3	622 M	7
4	155 M	10

2.4. **Smart fibre optic networks structural design.** The effectiveness of the smart fibre optic network needs to rely on the large-scale application of fibre optic remote coupling device, which consists of a sub-station system (fibre optic remote coupling device) and a master management system [25].

The master station sends data link connection commands to the fibre optic remote coupling device, and the fibre optic remote coupling device receives them and couples or unchains the fibre core. The sub-station system completes the functions of accessing the fibre core, switching the fibre route, optical testing, information collection and so on. The master station management system completes the fibre optic network resource management. The main function of the intelligent fiber optic network system is to obtain

the operation number information of the power communication equipment in real time, issue relevant commands, realize the controllable switching between the faulty fibre core and the standby fibre core, and monitor the operation status through the obtained information. The structure of intelligent optical fibre network based on optical fibre remote coupling technology is shown in Figure 3.

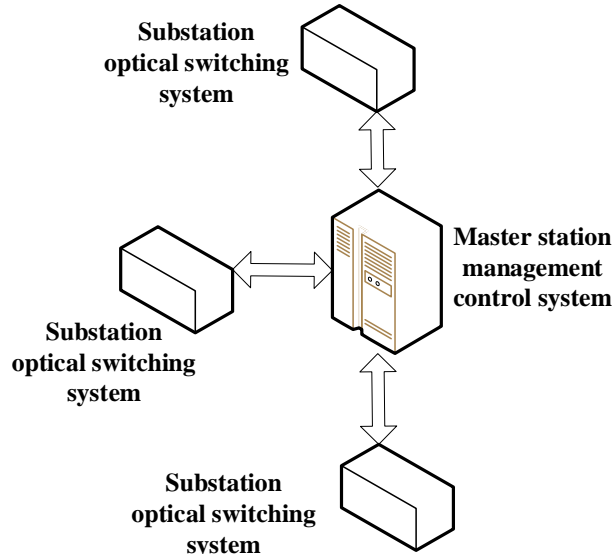


Figure 3. Intelligent fibre-optic network architecture

3. Optically coupled RF modulation format feature extraction.

3.1. five modulation formats. Most of the current experimental schemes based on feature extraction are more complex in structure, often have poor recognition performance under low signal-to-noise ratio conditions, and there exists a feature that can only discriminate between specific signals, i.e., for other classes of signals other features are required to discriminate. Therefore, in this work, a feature extraction scheme based on signal self-coherence is proposed for the feature extraction study of optically coupled signals. The feature extraction of this scheme is uniformly applicable.

Five common modulation formats are used [26,27], including 2ASK, BPSK, QPSK, 2FSK and LFM.

(1) 2ASK signal.

The mathematical expression for the 2ASK signal is shown below:

$$S_{2ASK} = Am(t) \cos(2\pi f_c t + \phi), (n-1)T_b \leq t \leq nT_b \quad (1)$$

where A is the amplitude, $m(t)$ is the unipolar binary baseband signal, f_c is the carrier frequency, ϕ is the initial phase, and T_b is the codeword width.

(2) 2FSK signal.

2FSK is known as Binary Frequency Shift Keying, the basic principle of this modulation format is to modulate the binary symbol 0 or 1 by changing the frequency of the carrier. 2FSK is achieved by switching between different frequencies for the transmission of bit streams, so 2FSK signals have a stronger noise immunity compared to 2ASK signals. The mathematical expression for 2FSK is shown below:

$$S_{2FSK} = Am(t) \cos(2\pi f_0 t) + A\bar{m}(t) \cos(2\pi f_1 t) \quad (2)$$

where f_0 and f_1 are two different frequencies, and $\bar{m}(t) = 1 - m(t)$.

(3) BPSK signal.

BPSK is known as Binary Phase Shift Keying, and the basic principle of this modulation format is to achieve binary 0 or 1 modulation by controlling the phase change of the signal. The mathematical expression of the BPSK signal is shown below:

$$S_{BPSK} = \begin{cases} A \cos(2\pi f_c t + 0), & a_n = 1 \\ A \cos(2\pi f_c t + \pi), & a_n = 0 \end{cases} \quad (3)$$

(4) QPSK signal.

The full name of QPSK is Quadruple Phase Shift Keying, both QPSK and BPSK signals transmit the binary symbol 0 or 1 through the phase, but QPSK further divides the phase into four equal parts. The mathematical expression of QPSK signal is shown below:

$$S_{QPSK}(t) = A \cos(2\pi f_c t + \varphi_n) \quad (4)$$

where φ_n is the modulated phase.

(5) LFM signal.

LFM signal is the full name of linear frequency modulation (LFM) signal, and the most important feature of LFM signal that distinguishes it from the above four signals is that LFM signal does not require a random coding sequence. However, the spectral width required for LFM signal is much larger than that of the above four signals. Assuming that the initial phase is 0, the mathematical expression of the LFM signal is shown below:

$$S_{LFM}(t) = A \cos[2\pi(f_m t + kt^2/2)], \quad 0 \leq t \leq T \quad (5)$$

where f_m is the frequency of the LFM signal at $t = 0$ and k is the rate of frequency change.

3.2. Signal pre-processing. Noise has a large interference to the signal, in order to reduce the interference of noise to the signal, this paper adds preprocessing to the sampled signal, including Hilbert transform, smoothing and power normalisation [28,29].

Firstly, the Hilbert transform is mainly used for filtering the signal. Secondly, the smoothing process can further bring out the features of the signal. Finally, the power normalisation process compresses all the data in the interval 0 to 1, which facilitates the later generation of histograms of amplitude statistics for deep learning. The statistical histogram is a complete statistical histogram of the sampled data from a number of signal cycles in a specific way. The advantage of using statistical histogram is that not only does it not require synchronisation of signals to demodulate the received signals, but it also reduces the cost of the communication system and has better reliability.

The vertical coordinates of the preprocessed sampled data are divided equally into one hundred equal parts, and the number of sampling points falling in each equal part are counted, and these sampling points are used to generate a new statistical graph. The horizontal coordinates of the new statistical graph are one hundred equal parts, and the vertical coordinates are the number of sampling points in each equal part, which is also called the amplitude statistical graph of the signal. The histogram generated after preprocessing is shown in Figure 4. It can be seen more clearly that the five modulation formats have significant shape differences after preprocessing.

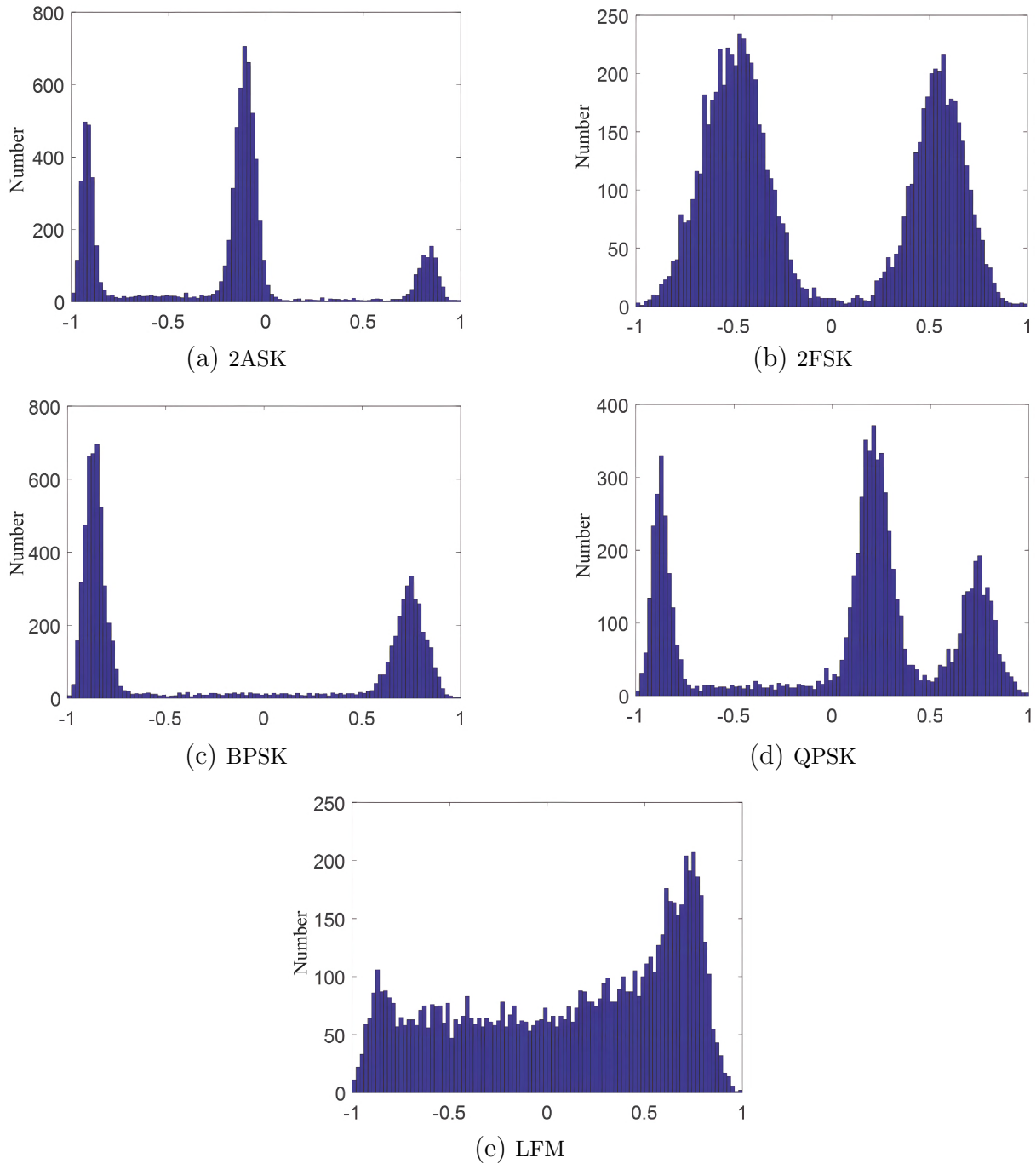


Figure 4. Histograms generated after pre-processing

4. CNN+LSTM based optical coupled RF modulation format identification.

4.1. **CNN.** The CNN is one of the core representative models of deep learning, and its model structure is mainly composed of convolutional layer, pooling layer and fully connected layer. The convolutional and pooling layers are mainly used for feature extraction of data in images, while the fully connected layer is mainly used for feature recognition and classification [30].

The convolution operation and pooling operation introduced in the CNN model have the function of feature extraction for the picture. The input picture of the CNN model can be a colour picture or a processed grey scale picture, which mainly depends on whether the colour has an effect on the picture information or not. If the colour has no effect on

the picture information, or can be ignored. In general, greyscale processing of coloured pictures is often required to reduce the computational complexity of the network structure. The Convolutional and Pooling layers are the feature extraction part of the CNN, where the Filter is also known as the Convolutional Kernel.

The feature mapping layer is calculated as follows:

$$F_{k,h} = f\left(\sum_{c=0}^{c-1} \sum_{m=0}^{d-1} \sum_{n=0}^{d-1} \omega_{m,n} x_{i+m,j+n} + b\right) \quad (6)$$

where d denotes the size of the convolution kernel, c denotes the depth of the input image, $F_{k,h}$ denotes the elements of the k -th row and h -th column in the feature mapping layer, and b denotes the bias value of the convolution kernel.

When other values are selected for the step size, the dimensions of the feature mapping layer are changed accordingly.

$$W_2 = (W_1 - F + 2P) / S + 1 \quad (7)$$

$$H_2 = (H_1 - F + 2P) / S + 1 \quad (8)$$

where W_1 denotes the width of the picture before the convolution operation, W_2 denotes the width of the picture of the feature mapping layer after the convolution operation, S denotes the step length of the move, P denotes the number of turns of the input picture to complement the zeros, H_1 denotes the height of the picture before the convolution operation, and H_2 denotes the height of the picture of the feature mapping layer after the convolution operation.

In the CNN model of this paper, it is easy to cause overfitting due to too many training parameters. In order to prevent overfitting, dropout is added to the CNN model to enhance the robustness of the training parameters, as shown in Figure 5. The basic principle of dropout is to stop participating in the network parameter computation with a probability p for the neurons of the added dropout layer during the training process, where the probability p can be set by human. This not only reduces the computational complexity of the network, at the same time, a reasonable dropout does not reduce the recognition correctness of the network, but rather improves the computational speed of the network.

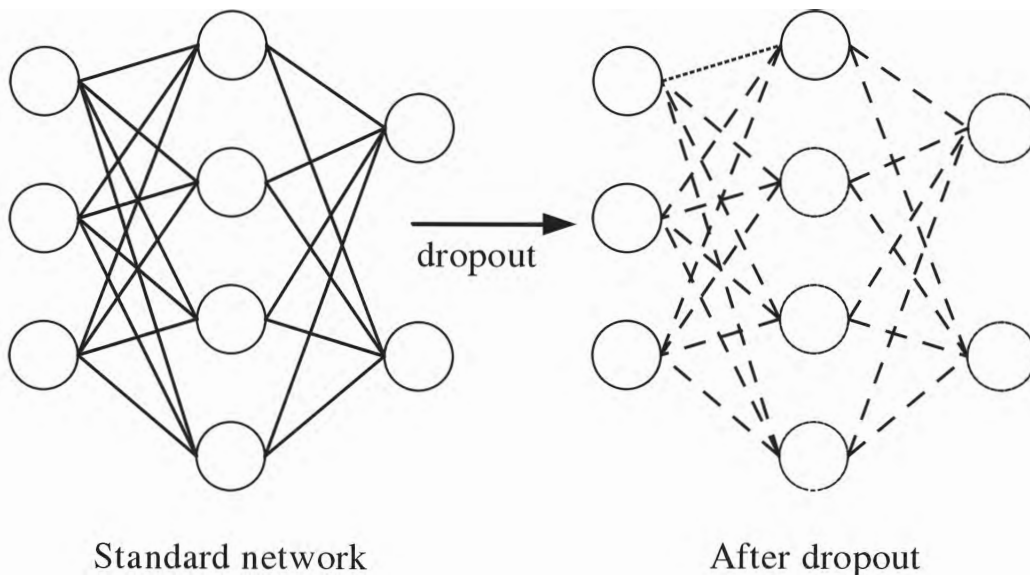


Figure 5. Dropout principle

With dropout the neurons (represented by dashed lines) are hidden and not involved in the computation in one forward propagation of the neural network, thus reducing the computational complexity of the network accordingly.

4.2. **LSTM.** The LSTM model is an improved model of the RNN model that avoids the gradient vanishing and gradient explosion problems in the RNN model [31]. To solve the gradient vanishing and gradient explosion problems, LSTM adds a new state c to the RNN model to hold the long-term state information. This new state is called the unit state and is expanded in time order as shown in Figure 6.

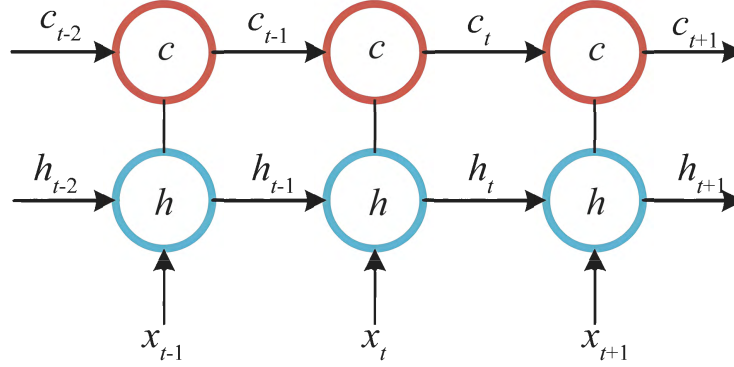


Figure 6. LSTM internal memory states

The model is built by introducing the concept of gates in the LSTM model. A gate is essentially a fully connected layer and the representation of a gate is similar to a BP neural network as shown below:

$$g(x) = f(Wx + b) \quad (9)$$

where f is the activation function, W is the weight matrix, x is the input vector and b is the bias.

In LSTM, the data in the cell state c is mainly controlled by the forgetting gate and the input gate. The expression of the forgetting gate is shown below:

$$f_t = \sigma_1(W_f \cdot [h_{t-1}, x_t] + b_f) \quad (10)$$

where σ_1 is the forgetting gate activation function, W_f is the weight matrix of the forgetting gate and b_f is the bias matrix of the forgetting gate.

The expression for the input gate is shown below:

$$i_t = \sigma_2(W_i \cdot [h_{t-1}, x_t] + b_i) \quad (11)$$

where σ_2 is the input gate activation function, W_i is the weight matrix of the input gate and b_i is the bias matrix of the input gate.

The expression for the currently entered unit status c' is shown below:

$$c'_t = \sigma_3(W_c \cdot [h_{t-1}, x_t] + b_c) \quad (12)$$

where σ_3 is the activation function of the current input cell state c' , W_c is the weight matrix of the current input cell state, and b_c is the bias matrix of the current input cell state.

The final output expression of LSTM is shown below:

$$h_t = o_t * \sigma_t(c_t) \quad (13)$$

where σ_t is the final output activation function.

4.3. Classification and recognition based on CNN+LSTM. The basic principle of CNN+LSTM model is to replace the fully connected layer in the traditional CNN model with LSTM model [32]. The structure of CNN+LSTM model is shown in Figure 7. The CNN is used to automatically learn the local features of the modulated signal and the LSTM learns the temporal features, and end-to-end training improves the performance of modulation format recognition.

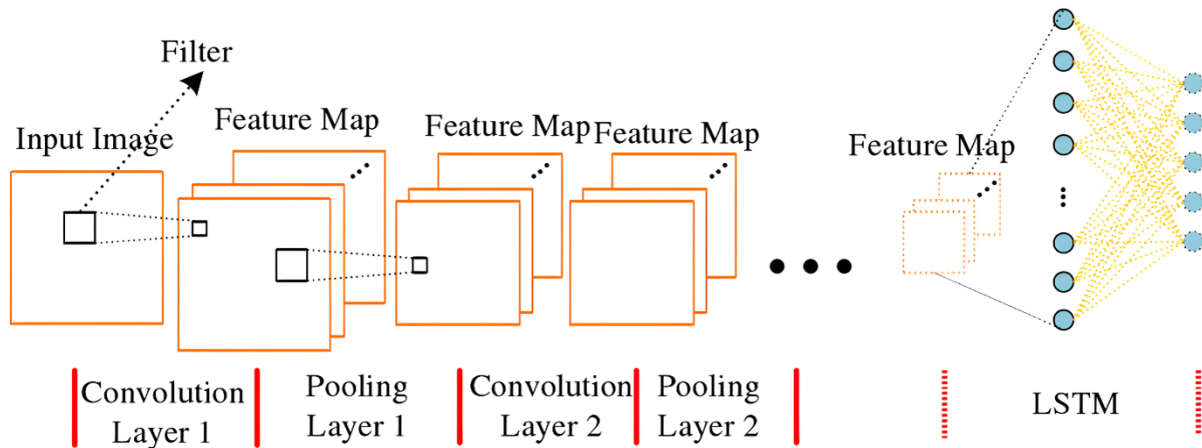


Figure 7. CNN+LSTM Models

Input layer: Receive complex IQ samples of the original modulated signal as input.

CNN layer: 1D convolutional layer is used to extract features from the input signal, the size of convolutional kernel is 3, the activation function is ReLU, the sampling method is strides, and the BatchNorm layer is used to accelerate the convergence.

Pooling layer: the temporal resolution of the feature map is reduced using a 1D maximal pooling layer with a pooling size of two.

LSTM layer: the CNN extracted features are fed into the LSTM layer to learn the temporal feature dependency, and the number of units is 128.

Fully Connected Layers: One or more fully connected layers are used to reduce the dimensionality, and finally a softmax classification layer is connected.

Output Layer: Outputs the predicted probabilities for different modulation formats.

Loss function: cross-entropy loss is used with Adam optimiser.

Model training: end-to-end training of CNN+LSTM model, using minibatch training, batchsize is 32.

In order to improve the quality of the received signal, this work adds preprocessing to the received signal and then generates 30 amplitude histograms. Therefore, the input neurons of the CNN+LSTM model are 30. The output neurons of the CNN+LSTM model are 5, which corresponds to five modulation formats, including 2ASK, BPSK, QPSK, 2FSK and LFM.

5. Experimental results and analyses.

5.1. Experimental data set. In this experiment, samples of five modulation formats are identified in the signal-to-noise ratio [-10dB, 15dB] range. The sample data is derived from the RadioML 2018 dataset. The sample data were divided into 3000 groups in total. Among them, 2500 sets of data were used as the training data for the CNN+LSTM model. In the training dataset, each histogram data has a label from 1 to 5, which corresponds to five modulation formats, namely BPSK, 2ASK, LFM, QPSK and 2FSK. In order to

test the recognition performance of the deep learning model, the remaining 500 sets of data are used as test data for the CNN+LSTM model.

5.2. Full network coverage analysis. In order to achieve full network coverage with the least number of sub-station terminals, three methods are investigated, namely the random distribution method, the longest distance first method, and the highest value first method.

(1) Completely random method. The random distribution method determines the full network coverage by randomly selecting sub-station nodes. After determining the sub-station, data links are constructed with other sub-stations, the amount of coverage value is calculated and removed from the fibre optic network, and then the next sub-station is randomly selected until the full network is covered.

(2) Longest distance first method. The longest distance priority method removes the sub-station with the largest distance value by calculating the coverage distance of all the sub-station nodes and repeating the above steps to remove all the sub-stations of the power communication in turn.

(3) Highest value priority method. The highest-value-first method is similar to the longest-distance-first method, with the difference that the principle for selecting a sub-station node is the amount of value of the fibre covered by the node. For the value amount of the fibre, this paper is mainly based on the importance of the optical path carried on the fibre, as shown in Table 4.

Table 4. Optical path importance

Optical Path Category	With second routing	Significance
Segment transmission systems	N	8
Segment Transmission Systems	Y	6
Provincial Network Transmission System (PNTS)	N	6
Provincial Network Transmission System (PNTS)	Y	4
Municipal transmission system	N	4
Municipal transmission system	Y	2

The amount of value of a fibre optic is defined as

$$V_i = L_i * \sum S_{ij} \quad (14)$$

where L_i is the length of fibre i and S_{ij} is the importance of the j -th optical path carried on fibre i .

In this paper, Matlab is used as a simulation platform to simulate and analyse the three strategies above and compare these optical fibre network full coverage strategies. The number of sub-station nodes required for full network coverage under the three strategies is tested using the number of nodes configured for different power communication full network nodes as a performance indicator, and the results are shown in Figure 8.

The experimental results show that the number of configured nodes of the three strategies increases with the increase in the number of nodes in the whole network of power communication, in which the completely random strategy grows faster and reaches 21 when the number of nodes in the whole network reaches 100. The number of configured nodes of the other two strategies increases slower and the curves are basically the same. The number of configured nodes for the two strategies is 14 and 13.5 respectively when the number of nodes in the whole network reaches 100. Comparison reveals that the number of configured nodes for the highest-value-first strategy is the smallest. Therefore, the highest-value-first strategy has a higher application value and possesses higher feasibility with the best network-wide coverage performance.

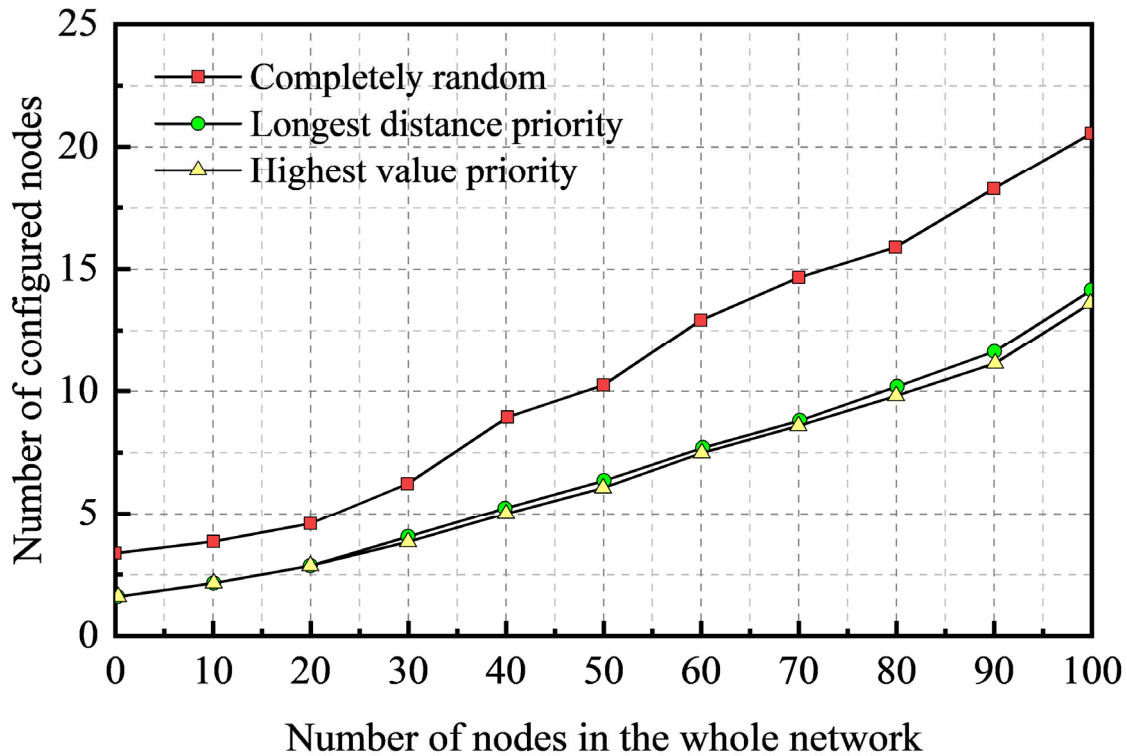


Figure 8. Comparison of three strategy simulations

5.3. Analysis of recognition results. The five modulation formats were classified and recognised using BP neural network, CNN, LSTM and CNN+LSTM in the signal-to-noise ratio [-10dB,15dB] interval, respectively. The main parameter settings of the five models are shown in Table 5.

Table 5. Main parameter settings for the five models

	BP neural network	CNN	LSTM	CNN+LSTM
Activation function	ReLU	ReLU	ReLU	ReLU
Probability function	Softmax	Softmax	Softmax	Softmax
Epoch	227	12	496	21
Number of hidden layer nodes	45	-	256	256

The recognition results of the four neural network models for the optically coupled RF modulation format are shown in Figure 9.

It can be seen that the CNN+LSTM model can effectively recognise the five selected RF signals. As the signal-to-noise ratio increases, the recognition rates of all four neural network models increase along with it. The BP neural network has the worst recognition, with an average recognition rate of 82% in the signal-to-noise ratio [-10dB, -1dB] interval. The CNN+LSTM model has the relatively highest recognition rate in the signal-to-noise ratio [-10dB, -1dB] interval, with an average recognition rate of 92.7%.

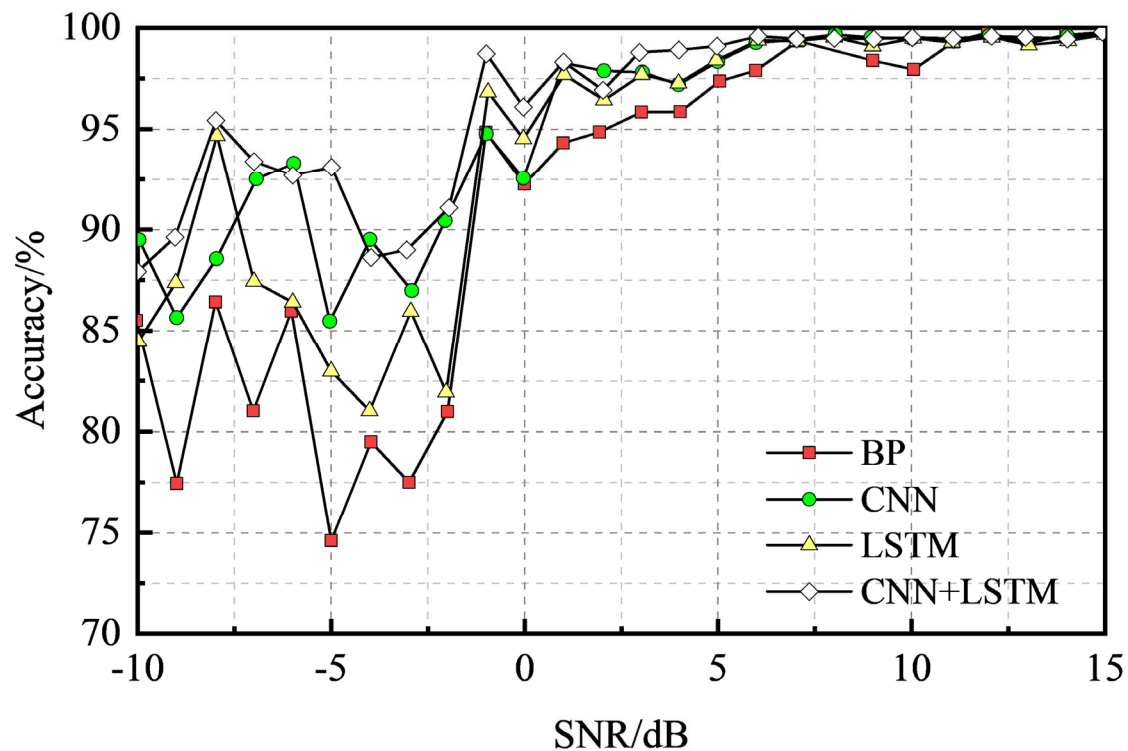


Figure 9. Recognition rates for five modulation formats

6. Conclusion. In order to effectively improve the efficiency of communication fibre optic network operation and maintenance and to achieve intelligent operation and maintenance, this work analyses the analysis of existing intelligent optical network technologies and uses the histogram of amplitude statistics of optically coupled RF signals as an input to the CNN+LSTM model to achieve the classification and identification of five modulation formats (2ASK, BPSK, QPSK, 2FSK and LFM). Finally, BP neural network, CNN, LSTM and CNN+LSTM were tested for comparison using RadioML 2018 dataset. The results show that the CNN+LSTM model has the relatively highest recognition rate in the signal-to-noise ratio [-10dB, -1dB] interval, with an average recognition rate of 92.7%, which greatly improves the recognition correctness of RF signals under low signal-to-noise ratio conditions. Follow-up studies will try more complex CNN network structures, such as residual networks (ResNet) and densely connected networks (DenseNet), to learn more abstract and discriminative features.

REFERENCES

- [1] T.-Y. Wu, Y.-Q. Lee, C.-M. Chen, Y. Tian, and N. A. Al-Nabhan, "An enhanced pairing-based authentication scheme for smart grid communications," *Journal of Ambient Intelligence and Humanized Computing*, 2021. [Online]. Available: <https://doi.org/10.1007/s12652-020-02740-2>
- [2] Y. Ma, Y. Peng, and T.-Y. Wu, "Transfer learning model for false positive reduction in lymph node detection via sparse coding and deep learning," *Journal of Intelligent & Fuzzy Systems*, vol. 43, no. 2, pp. 2121-2133, 2022.
- [3] S.-M. Zhang, X. Su, X.-H. Jiang, M.-L. Chen, T.-Y. Wu, "A traffic prediction method of bicycle-sharing based on long and short term memory network," *Journal of Network Intelligence*, vol. 4, no. 2, pp. 17-29, 2019.
- [4] H. M. Hasanien, and A. A. El-Fergany, "Salp swarm algorithm-based optimal load frequency control of hybrid renewable power systems with communication delay and excitation cross-coupling effect," *Electric Power Systems Research*, vol. 176, p. 105938, 2019.

- [5] K.-K. Tseng, C. Wang, T. Xiao, C.-M. Chen, M. M. Hassan, and V. H. C. de Albuquerque, "Sliding large kernel of deep learning algorithm for mobile electrocardiogram diagnosis," *Computers & Electrical Engineering*, vol. 96, p. 107521, 2021.
- [6] E. K. Wang, C.-M. Chen, M. M. Hassan, and A. Almogren, "A deep learning based medical image segmentation technique in Internet-of-Medical-Things domain," *Future Generation Computer Systems*, vol. 108, pp. 135-144, 2020.
- [7] A. Kwasinski, F. Andrade, M. J. Castro-Sitiriche, and E. O'Neill-Carrillo, "Hurricane Maria effects on Puerto Rico electric power infrastructure," *IEEE Power and Energy Technology Systems Journal*, vol. 6, no. 1, pp. 85-94, 2019.
- [8] X. Huang, H. Xiong, J. Chen, and M. Yang, "Efficient Revocable Storage Attribute-based Encryption with Arithmetic Span Programs in Cloud-Assisted Internet of Things," *IEEE Transactions on Cloud Computing*, vol. 11, no. 2, pp. 1273-1285, 2023.
- [9] H. Xiong, T. Yao, H. Wang, J. Feng, and S. Yu, "A Survey of Public-Key Encryption with Search Functionality for Cloud-Assisted IoT," *IEEE Internet of Things Journal*, vol. 9, no. 1, pp. 401-418, 2022.
- [10] H. Xiong, Y. Wu, C. Jin, and S. Kumari, "Efficient and Privacy-Preserving Authentication Protocol for Heterogeneous Systems in IIoT," *IEEE Internet of Things Journal*, vol. 7, no. 12, pp. 11713-11724, 2020.
- [11] R. V. Yohanandhan, R. M. Elavarasan, P. Manoharan, and L. Mihet-Popa, "Cyber-physical power system (CPPS): A review on modeling, simulation, and analysis with cyber security applications," *IEEE Access*, vol. 8, pp. 151019-151064, 2020.
- [12] W. S. Saif, M. A. Esmail, A. M. Ragheb, T. A. Alshawi, and S. A. Alshebeili, "Machine learning techniques for optical performance monitoring and modulation format identification: A survey," *IEEE Communications Surveys & Tutorials*, vol. 22, no. 4, pp. 2839-2882, 2020.
- [13] D. S. Shakya, "Machine learning based nonlinearity determination for optical fiber communication-review," *Journal of Ubiquitous Computing and Communication Technologies*, vol. 1, no. 2, pp. 121-127, 2019.
- [14] H. Liu, J. Ma, T. Xu, W. Yan, L. Ma, and X. Zhang, "Vehicle detection and classification using distributed fiber optic acoustic sensing," *IEEE Transactions on Vehicular Technology*, vol. 69, no. 2, pp. 1363-1374, 2019.
- [15] C. Du, S. Dutta, P. Kurup, T. Yu, and X. Wang, "A review of railway infrastructure monitoring using fiber optic sensors," *Sensors and Actuators A: Physical*, vol. 303, p. 111728, 2020.
- [16] X. Zhu, B. Liu, X. Zhu, J. Ren, R. Ullah, Y. Mao, X. Wu, M. Li, S. Chen, and Y. Bai, "Transfer learning assisted convolutional neural networks for modulation format recognition in few-mode fibers," *Optics Express*, vol. 29, no. 22, pp. 36953-36963, 2021.
- [17] Z. Zhang, M. Zhu, Y. Li, Y. Li, and S. Wang, "Joint recognition and parameter estimation of cognitive radar work modes with LSTM-transformer," *Digital Signal Processing*, vol. 140, p. 104081, 2023.
- [18] A. M. Alatwi, A. N. Z. Rashed, and I. A. Abd El Aziz, "High speed modulated wavelength division optical fiber transmission systems performance signature," *Telkommnika*, vol. 19, no. 2, pp. 380-389, 2021.
- [19] I. Amiri, A. N. Z. Rashed, and P. Yupapin, "High-speed light sources in high-speed optical passive local area communication networks," *Journal of Optical Communications*, vol. 44, no. 1, pp. 61-67, 2023.
- [20] J. Zhao, Y. Liu, and T. Xu, "Advanced DSP for coherent optical fiber communication," *Applied Sciences*, vol. 9, no. 19, p. 4192, 2019.
- [21] J. Logeshwaran, M. Ramkumar, T. Kiruthiga, and R. Sharanpravin, "The role of integrated structured cabling system (ISCS) for reliable bandwidth optimization in high-speed communication network," *Journal on Communication Technology*, vol. 13, no. 1, pp. 2635-2639, 2022.
- [22] B. J. Puttnam, G. Rademacher, and R. S. Luís, "Space-division multiplexing for optical fiber communications," *Optica*, vol. 8, no. 9, pp. 1186-1203, 2021.
- [23] M. Matsuura, H. Nomoto, H. Mamiya, T. Higuchi, D. Masson, and S. Fafard, "Over 40-W electric power and optical data transmission using an optical fiber," *IEEE Transactions on Power Electronics*, vol. 36, no. 4, pp. 4532-4539, 2020.
- [24] L. Yu, Z. Liu, M. Wen, D. Cai, S. Dang, Y. Wang, and P. Xiao, "Sparse code multiple access for 6G wireless communication networks: Recent advances and future directions," *IEEE Communications Standards Magazine*, vol. 5, no. 2, pp. 92-99, 2021.

- [25] T. Sasai, M. Nakamura, E. Yamazaki, S. Yamamoto, H. Nishizawa, and Y. Kisaka, "Digital longitudinal monitoring of optical fiber communication link," *Journal of Lightwave Technology*, vol. 40, no. 8, pp. 2390-2408, 2021.
- [26] S. Ranathive, K. Vinoth Kumar, A. N. Z. Rashed, M. S. F. Tabbour, and T. Sundararajan, "Performance signature of optical fiber communications dispersion compensation techniques for the control of dispersion management," *Journal of Optical Communications*, vol. 43, no. 4, pp. 611-623, 2022.
- [27] Z. Qi, Y. Li, Y. Huang, J. Feng, Y. Zheng, and X. Chen, "A 15-user quantum secure direct communication network," *Light: Science & Applications*, vol. 10, no. 1, p. 183, 2021.
- [28] M. Pankratova, A. Vasylychenkova, S. A. Derevyanko, N. B. Chichkov, and J. E. Prilepsky, "Signal-noise interaction in optical-fiber communication systems employing nonlinear frequency-division multiplexing," *Physical Review Applied*, vol. 13, no. 5, p. 054021, 2020.
- [29] D. P. Karuppusamy, "Mimo based high speed optical fiber communication system," *Journal of Electronics and Informatics*, vol. 1, no. 2, pp. 107-116, 2019.
- [30] T. Kattenborn, J. Leitloff, F. Schiefer, and S. Hinz, "Review on Convolutional Neural Networks (CNN) in vegetation remote sensing," *ISPRS Journal of Photogrammetry and Remote Sensing*, vol. 173, pp. 24-49, 2021.
- [31] W. Lu, J. Li, Y. Li, A. Sun, and J. Wang, "A CNN-LSTM-based model to forecast stock prices," *Complexity*, vol. 2020, pp. 1-10, 2020.
- [32] W. Lu, J. Li, J. Wang, and L. Qin, "A CNN-BiLSTM-AM method for stock price prediction," *Neural Computing and Applications*, vol. 33, pp. 4741-4753, 2021.